Performance improvement of Predictive Control methods of MPDTC Strategies for Electrical Drives using multilevel inverter

Mr.Suraj R Karpe1

, Prof.Mithun G Aush

Assistant Professor, Electrical Engineering, S.B.Patil College of Engineering, Indapur, Maharashtra, India 1
Assistant Professor, Electrical Engineering, CSMSSCS College of Engineering, Aurangabad,Maharashtra , India 2

***Abstract*— In Power Electronics, Predictive Current control (PCC) and Predictive Torque control (PTC) methods are advanced control strategy. To control a Permanent Magnet Synchronous motor machine (PMSM) or induction machine (IM), the predictive torque control (PTC) method evaluates the stator flux and electromagnetic torque in the cost function and Predictive Current control (PCC) [1] considers the errors between the current reference and the measured current in the cost function. The switching vector selected for the use in IGBTs minimizes the error between the references and the predicted values. The system constraints can be easily included [4, 5]. The weighting factor is not necessary. Both the PTC and PCC methods are most useful direct control methods with PMSM method gives 10% to 30% more torque than an induction motor also not require modulator [3]. Induction motor work on only lagging power factor means it can produce only 70-90% of torque produced by PMSM with same current. PCC and PTC method with 15-level H-bridge multilevel inverter using PMSM reduces 23% more THD in torque, speed and stator current compared to PCC and PTC method with 15-level H-bridge multilevel inverter using induction motor [21]. Switching losses are minimized because the transistors are only switched when it is needed to keep torque and flux within their bounds. The switching pattern of semiconductor switches used to get better performance of multilevel inverter. In this paper, the PTC and PCC methods with 15-level H-bridge multilevel inverter using PMSM and IM are carried out; gives excellent torque and flux responses, robust, and stable operation achieved compared to the PTC and PCC methods with 2-level voltage source inverter. This novel method attracted the researchers very quickly due to its straightforward algorithm and good performances both in steady and transient states [8].**

***Index Terms*— Electrical drives, predictive current control (PCC), predictive torque control (PTC), Permanent Magnet Synchronous Motor (PMSM), Induction Motor, 15-level H-Bridge multilevel inverter, Voltage Source Inverter (VSI).**

I. INTRODUCTION

Predictive Current control (PCC) and Predictive Torque control (PTC) methods are promising methods. Along reducing torque ripples, the FCS-PTC method also illustrates a number of advantages, like the easy inclusion of constraints, easy implementation, straightforward, algorithm and fast dynamic responses. The basic concept of model predictive direct torque control (MPDTC) method is to calculate the required control signals in advance [6]. In the MPDTC

Method, pulse width modulation is needless. The inverter model is required in the control method. During MPDTC, the PTC and PCC method calculates all possible voltage vectors within one sampling interval and selects the best one by using an optimization cost function [7]. To date, the PCC and PTC methods have been adapted in many operational situations and widely investigated, as given in the articles [8], [9].

Model predictive control (MPC) in recent years has received convincingly contemplation and has gained demand in the power electronics and industrial drives association. This MPC control strategy was first introduced in 1970, developed for process control applications, is used commonly in the industry with numerous applications reported [4]. The basic perception of model predictive control methods is that the decision of the controller is not centered on past state of the system, but with the predicted behavior of the state variables and proper selection of the controlled variables either offline or online. MPC is also referred as receding horizon control, as where its main perception is to reflect an infinite prediction horizon by constantly sliding the prediction horizon. The current expansion and new orientation in the area of MPC mentioned in [5]. Due to simple in concept, the MPC also sometimes used to control the power converters because of its computational complexity is a burden to the processors. Now a day due to the evolution of new high speed processor, the usage of MPC became an increase. In [6] the MPC is used to control a VSI and multilevel inverter, where a discrete-time model of the VSI used to predict the forthcoming value of the load current for all possible voltage vectors generated by the inverter. According to this, MPC has been widely used in many applications in power electronics such as controlling various industrial drives like DC-DC converters [7], in matrix converters [8]. MPDTC can be also used for speed control Permanent magnet synchronous motor and induction motor [9] [10] based on a linearized state-space representation that describes the dynamic operation.

When MPC compared with the DTC method, the PTC method has two demerits: depend on speed and require higher calculation time. Due to the implementation of the optimal cost function, the PTC method takes more time; this problem can be solved easily, with better and faster microprocessing unit [10], [11]. The conventional PTC method for induction machine (IM) and PMSM motor applications demands the rotor electrical speed in the prediction steps. The predicted stator current values are dependent on the estimated speed and also on measured values of speed.

Now a day, if a semiconductor switch is directly connected to the system with Medium sized voltage grids will create problems. To solve this problem, a multilevel inverter topology has been introduced as an alternative solution for medium voltage and high voltage and extra high voltage power situations. A multilevel inverter can be used renewable energy as a source and can achieve high power rating. So, solar, fuel cells and wind like renewable energy sources can be easily interfaced to a multilevel inverter structure for a high power application. The multilevel inverter concept has been used for past three decades. Multilevel inverter (MLI) has become more popular over the year and magnetized considerable affection in recent years. MLI generating a stepped voltage waveform which has compressed the harmonic distortion because of inclusion a group of power semiconductor devices and capacitor as voltage sources. The number of merits of MLI is its ability to reduce voltage stress on power switches, dv/dt ratio and common mode voltage, thus improving the quality of the output [1]. There are various topologies of MLI such as Diode Clamped Multilevel Inverter, Cascaded Multilevel Inverter and Flying Capacitor Multilevel Inverter. Out of which H-Bridge multilevel inverter has various advantages such as generate output voltages with extremely low distortion, and lower and draw input current with very low distortion, generate smaller common-mode (CM) voltage, thus reducing the stress on the motor bearings and can operate with a lower switching frequency.

In this paper, the PTC and PCC methods with 15-level H-bridge multilevel inverter using PMSM and IM are carried out by simulation method and compared with the PTC and PCC methods with 2-level voltage source inverter. PCC and PTC method with 15-level H-bridge multilevel inverter using PMSM reduces 23% THD in torque, speed and stator current compared to PCC and PTC method with 15-level H-bridge multilevel inverter using an induction motor [10] [21]. In this paper, switching loses minimization technique through THD minimization. Switching losses are minimized because the transistors are only switched when it is needed to keep torque and flux within their bounds. This novel method attracted the researchers very quickly due to its straightforward algorithm and good performances both in steady and transient states [8].

II. MODELING OF PMSM

Here, with the help of the model of the synchronous machine without damper winding and field current dynamics, the mathematical model for the vector control of the PMSM have derived with its dynamic d-q model. The synchronously rotating rotor reference frame is used so that stator winding quantities is transformed to the synchronous rotating reference frame that is revolving at rotor speed. The model of PMSM without damper winding has been developed in the rotor reference frame using assumptions as Saturation is neglected, induced EMF is sinusoidal, core losses are negligible, there are no field current dynamics. It is also be considered that rotor flux is constant at a given operating point and concentrated along the d-axis while there is zero flux along the q-axis, an assumption similarly made in the derivation of indirect vector controlled induction motor drives. With the help of a rotor reference frame, can determine independently of the stator voltages and currents, the instantaneous induced emf and subsequently the stator currents and torque of the machine when the position of the rotor magnets is considered. When a rotor reference frame is considered, it means the equivalent q- and d- axis stator windings are transformed to the reference frames that are revolving at rotor speed. The residue is that there is a zero speed differential between the rotor and stator magnetic fields and the stator q- and d- axis windings have a fixed phase relationship with the rotor magnet axis which is the d-axis in the modelling [17,18].

The mathematical model of a PMSM given by complex equations in the rotor reference frame is as below:
Voltage equations are given by:

$$V_d = R_s i_d - \omega_r \lambda_q + \frac{d\lambda_d}{dt} \quad [1]$$

$$V_q = R_s i_q - \omega_r \lambda_d + \frac{d\lambda_q}{dt} \quad [2]$$

Flux linkage is given by

$$\lambda_q = L_q i_q \quad [3], \qquad \lambda_d = L_d i_d + \lambda_f \quad [4]$$

Substituting Equation 3 and 4 in 1 and 2, we get,

$$V_q = R_s i_q - \omega_r \left(L_d i_d + \lambda_f\right) + \frac{d(L_q i_q)}{dt} \quad [5]$$

$$V_d = R_s i_d - \omega_r L_q i_q . + \frac{d}{dt}\left(L_d i_d + \lambda_f\right) \quad [6]$$

Arranging equation 5 and 6 in matrix form,

$$\begin{pmatrix} V_q \\ V_d \end{pmatrix} = \begin{pmatrix} R_s + \frac{dL_q}{dt} & \omega_r L_d \\ -\omega_r L_q & R_s + \frac{dL_d}{dt} \end{pmatrix} \begin{pmatrix} i_q \\ i_d \end{pmatrix} + \begin{pmatrix} \omega_r \lambda_f \\ \frac{d\lambda_f}{dt} \end{pmatrix} \quad [7]$$

The developed motor torque is being given by

$$T_e = \frac{3}{2}\left(\frac{P}{2}\right)\left(\lambda_d i_q - \lambda_q i_d\right) \quad [8]$$

$$T_e = \frac{3}{4} P\left[\lambda_f i_q + \left(L_d - L_q\right) i_q i_d\right] \quad [9]$$

$$T_e = T_L + B\omega_m + J\frac{d\omega_m}{dt} \quad [10]$$

Solving for rotor mechanical speed from equation 10, we get,

$$\omega_m = \int \left(\frac{T_e - T_L - B\omega_m}{J}\right) dt \quad [11]$$

And rotor electrical speed is

$$\omega_r = \omega_m \left(\frac{P}{2}\right) \quad [12]$$

III. Cascaded H-bridge multilevel inverter

A single-phase configuration of *n*-level H-bridge cascaded inverter is depicted in Fig.1. Each separate DC source is connected to a single-phase full-bridge/or H-bridge, inverter. Each inverter can generate three different voltage level outputs, $+V_{dc}$, 0, and $-V_{dc}$ by connecting the DC source to the AC output by different combinations of the four switches, S_1, S_2, S_3, and S_4. To obtain voltage level $+V_{dc}$, switches S_1 and S_4 turned on, whereas for voltage level $-V_{dc}$ switches S_2 and S_3 turned on. Zero level voltage can obtain by turning on switches S_1 and S_2 or S_3, and S_4. AC outputs of each synthesized different full-bridge inverter levels are connected in series for summing up to generate the multilevel voltage waveform. The number of output phase voltage *n*-levels in a cascade inverter defined by $n = 2l+1$, where *l* is the number of separate DC sources. As example phase voltage waveform for *n*-level cascaded H-bridge inverter with (*n*-1) /2 separate DC sources and (*n*- 1)/2 full bridges.

The output phase voltage generalized use as

$$v = v_{a1} + v_{a2} + v_{a3} + v_{a4} + v_{a5} \ldots\ldots\ldots + v_{an} \quad [13]$$

The Fourier transform of the corresponding stepped waveform follows [9, 5]:

$$V(\omega t) = \frac{4V_{dc}}{\pi} \sum [\cos(n\theta_1) + \cos(n\theta_2) + \cdots + \cos(n\theta_l)] \frac{\sin(n\omega t)}{n} \quad [14]$$

where n = 1,3,5,7.

By choosing conducting angles, θ_1, θ_2,……,θ_l, such that the total harmonic distortion (THD) is minimized. Predominately,

these conduction angles for suppressing lower frequency harmonics of 5th, 7th, 11th, and 13th,… orders are eliminated in output [10]. The main benefits and drawbacks of cascaded H-bridge multilevel converters are briefly summarized as follows [23]:

Benefits:

- The number of possible output voltage levels is more than twice the number of DC sources ($n = 2l+1$).
- The series of H-bridges makes for modularized layout and packaging. Enable the manufacturing process to be done faster and cheaper.

Drawbacks:

- Separate DC sources required for each of the H-bridges and could generate oscillating DC source power.Units

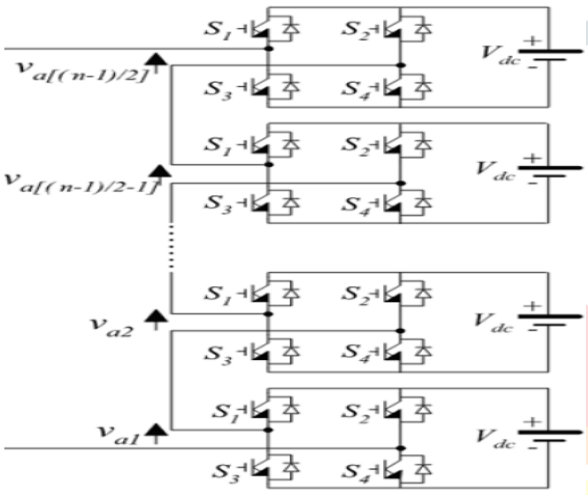

Fig. 1: Single leg of *n*-level cascaded H-bridge multilevel converter structure.

IV. Switching Losses

The losses in the semiconductors can be divided into two parts, namely switching losses (arising when the devices are switched on or off) and conduction losses (due to the ohmic resistance). These losses depend on the applied voltage, the commutated current and the semiconductor characteristics. Observing that in a VSI inverter, the voltage seen by each semiconductor is always half the total DC-link voltage leads to the Ideal switch turn-on (energy) loss

$$E_{on} = e_{on}\frac{1}{2}V_{dc}i_{ph} \quad [15]$$

Where e_{on} is a coefficient and i_{ph} is the phase current. For the Ideal switch, turn-off losses, a corresponding equation results with the coefficient e_{off}. Typically, e_{off} is an order of magnitude larger than eon. For a diode, the switch-on losses are effectively zero. The turn-off losses, however, which are reverse recovery losses, are linear in the voltage, but nonlinear in the commutated phase current. Similar to the switching losses, the conduction losses also depend on the applied voltage and the phase current. The DC link voltage is constant despite the neutral point fluctuations. The phase current is the sum of the current ripple and the fundamental component, which in turn depends only on the operating point given by the torque and the speed, but not on the switching pattern. Since the ripple is small compared to the fundamental current (typically in the range of 10% for a 3-level inverter), the conduction losses can be considered to be independent of the switching pattern.

V. Voltage Source Inverter

In this work, a two-level voltage source inverter is also applied to PTC and PCC methods. The topology of the inverter and its feasible voltage vectors are presented in Fig. 2. The switching state S can be expressed by the following vector:

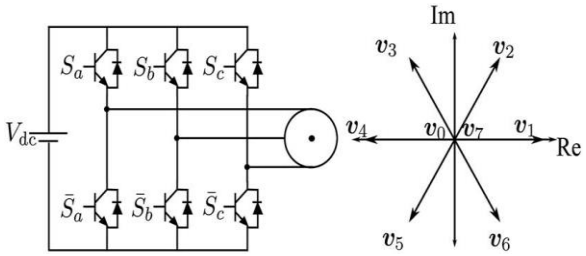

Fig. 2. *Left*: two-level voltage source inverter; *right*: voltage vectors

The stator voltage space vector representing the eight voltage vectors can be shown by using the switching states and the DC-link voltage,V_{dc} as:

$$V_s(S_a, S_b, S_c) = \left(\frac{2}{3}\right)V_{dc}\left(V_a + V_b e^{j\left(\frac{2}{3}\right)} + V_c e^{j\left(\frac{4}{3}\right)}\right) \quad [16]$$

Where V_{dc}, is the DC-link voltage and the coefficient of 2/3 is the coefficient comes from the Park's Transformation. The equation can be derived by using the line-to-line voltages of the AC motor which can be expressed as:

$$V_{ab} = V_{dc}(S_a - S_b) \quad [17]$$
$$, V_{bc} = V_{dc}(S_b - S_c) \quad [18]$$
$$V_{ca} = V_{dc}(S_c - S_a) \quad [19]$$

The stator phase voltages (line-to-neutral voltages) are required & can be obtained from the line-to-line voltages as.

$$V_a = (V_{ab} - V_{ca})/3 \quad [20]$$
$$, V_b = (V_{bc} - V_{ab})/3 \quad [21]$$
$$, V_c = (V_{ca} - V_{bc})/3 \quad [22]$$

If the line-to-line voltages in terms of the DC-link voltage, *Vdc*, and switching states are substituted into the stator phase voltages it gives:

$$V_a = \left(\frac{1}{3}\right)V_{dc}(2S_a - S_b - S_c) \quad [23]$$
$$V_b = \left(\frac{1}{3}\right)V_{dc}(-S_a + 2S_b - S_c) \quad [24]$$
$$V_a = \left(\frac{1}{3}\right)V_{dc}(-S_a - S_b + 2S_c) \quad [25]$$

The equation can be summarized by combining as:

$$V_a = Re(V_s) = \left(\frac{1}{3}\right)V_{dc}(2S_a - S_b - S_c) \quad [26]$$
$$V_b = Re(V_s) = \left(\frac{1}{3}\right)V_{dc}(-S_a + 2S_b - S_c) \quad [27]$$
$$V_c = Re(V_s) = \left(\frac{1}{3}\right)V_{dc}(-S_a - S_b + 2S_c) \quad [28]$$
$$S = \frac{2}{3}(S_a + aS_b + a^2S_c) \quad [29]$$

where $a = e^{j\frac{2\pi}{3}}$, $S_i = 1$ meansS_i ON, $\bar{S}_i$ means OFF, and $i = a, b, c$. The voltage vector V is related to the switching state S by:

$$v = V_{dc}S \quad [30]$$

where V_{dc} is the DC-link voltage

VI. PREDICTIVE DIRECT CONTROL METHODS FOR PMSM

A.PREDICTIVE CURRENT CONTROL (PCC)

Predictive Current Control (PCC) uses only the predicted stator currents in the stationary reference frame in order to control the multiphase drive. Current references are obtained in the rotating reference frame from an outer PI

speed control loop and a constant d-component current and then mapped in the stationary reference frame in order to be used in the cost function, as shown in Fig. 3. This simple predictive controller scheme has been implemented in multiphase drives, with different number of windings [10].

Fig.3 MPC based Predictive Current Control with an outer speed control loop

The aim is to generate a desired electric torque, which implies sinusoidal stator current references in a-b-c phase coordinates. In the stationary α-β-x-y reference frame, the control aim is traduced into a reference stator current vector in the α-β plane, which is constant in magnitude, but changing its electrical angle following a circular trajectory, and depending on the implemented multiphase machine, either null or non-null reference stator current vector in the x-y plane.

The PMSM model, stator current is as below:

$$i_s = -\frac{1}{R_\sigma}\left(\left(L_\sigma.\frac{di_s}{dt} - K_r.\left(\frac{1}{\tau_r} - j.\omega\right).\varphi_r\right) - v_s\right) \quad [31]$$

where $K_r = \frac{L_m}{L_r}, R_\sigma = R_s + K_r^2.R_r \; and \; L_\sigma = \sigma.L_s$

The forward Euler discretization is considered to predict the next step value as

$$\frac{dx}{dt} \cong \frac{x(k+1)-x(k)}{T_s} \quad [32]$$

where T_s is the sampling time of the system.

Using (8) and (9), the stator current can be predicted as

$$\bar{\imath}_s(k+1) = \left(1 - \frac{T_s}{T_\sigma}\right).i_s(k) + \frac{T_s}{T_\sigma}.\frac{1}{R_\sigma}.\left[K_r.\left(\frac{1}{T_r} - j.\omega(k)\right).\varphi_r(k) + v_s(k)\right] \quad [33]$$

$$where \; T_\sigma = \sigma.\frac{L_s}{R_\sigma}$$

The cost function is represented as below:

$$g_j = \sum_{h=1}^{N}\left\{\left|i_\alpha^* - i_\alpha(k+h)_j\right| + \left|i_\beta^* - i_\beta(k+h)_j\right|\right\} \quad [34]$$

From (11), to complete the design of the PCC method, the current reference generation is needful. In Fig. 2, the block diagram of the PCC method is illustarate. The torque reference is generated by a speed PI controller, and the reference of rotor flux magnitude is considered as a constant value.

The corresponding reference values for the field- and torque-producing currents i_d^* and i_q^* are produced by

$$i_d^* = \frac{|\varphi_r|^*}{L_m} \; [35], \qquad i_q^* = \frac{2}{3}\frac{L_r}{L_m}\frac{T^*}{|\varphi_r|^*} \quad [36]$$

In the cost function, the state's current values in $\alpha\beta$ frame are required. The inverse Park transformation is presented to satisfy this requirement as follows:

$$\begin{pmatrix}\alpha\\ \beta\end{pmatrix} = \begin{pmatrix}cos(\theta) & -sin(\theta)\\ sin(\theta) & cos(\theta)\end{pmatrix}\begin{pmatrix}d\\ q\end{pmatrix} \quad [37]$$

B.PREDICTIVE TORQUE CONTROL (PTC)

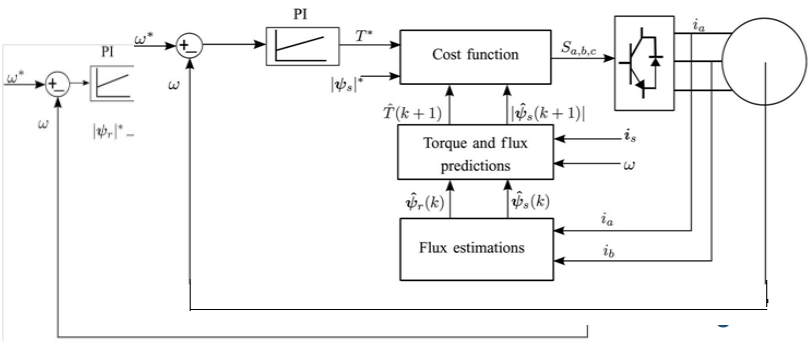

Fig.4 MPC based Predictive Torque Control with an outer speed control loop.

Predictive Torque Control (PTC) based on FCS-MPC for three phase two-level induction motor drives given in [20] is shown in Fig. 4. It is done by an outer PI based speed control and an inner PTC and controlled variables are the stator flux and torque. Torque reference is provided by an external PI, based on the speed error, while the stator flux reference has been set at its nominal value for base speed operation**.** Then the cost function (10) is evaluated and the switching state with a lower cost (J) is applied to the VSI. In order to improve PTC performance in [17] a modified cost function was presented, aimed to not only control stator flux and produced torque but also limit the maximum achievable α-β stator currents to ($i\alpha\beta{-}MAX$) and reducing harmonic components in the x-y plane.

The core aspects of PTC are the torque and flux predictions and the design of a cost function.

In the predictive algorithm, the next-step stator flux ˆ $\psi s(k+1)$ and the electromagnetic torque ˆ $T(k+1)$ must be calculated. By using (9) to discretize the voltage model (1), the stator flux prediction can be obtained as

$$\bar{\varphi}_s(k+1) = \varphi_s(k) + T_s.v_s(k) - R_s.T_s.i_s(k) \quad [38]$$

The electromagnetic torque can be

$$\bar{T}(k+1) = \frac{3}{2}.p.Im\{\bar{\varphi}_s(k+1)^*.\bar{\imath}_s(k+1)\} \quad [39]$$

The classical cost function for the PTC method is

$$g_j = \sum_{h=1}^{N}\left\{\left|T^* - \bar{T}(k+1)_j\right| + \lambda.\left|\|\varphi_s^*\| - \left\|\bar{\varphi}_s(k+h)_j\right\|\right|\right\} \quad [40]$$

VII. Results:

A.PCC and PTC method with PMSM and IM using15-level inverter:

PCC and PTC for a 4-pole induction machine have simulated with 15-level multilevel inverter and compared with 2-level voltage source inverter. The rating of induction motor is 5HP, 440V, 50Hz, 1440 RPM star connected induction motor. For all simulations, the motor characteristics will be utilized as below:

Stator Resistance (ohm)	= 1.403
Rotor Resistance (ohm)	= 1.395
Stator Self Inductance (H)	= 0.005839
Rotor Self Inductance (H)	= 0.005839
Mutual Inductance (H)	= 0.2037
No. of poles	= 4
Moment of Inertia (kg.m^2)	= 0.0005
Sampling time,	= 1 Sec

Table. 1: Induction motor parameters

PCC and PTC for a 4-pole PMSM have simulated with 15-level multilevel inverter and compared with 2-level voltage source inverter. For all simulations, the motor characteristics will be utilized as below: The parameters of PMSM motor are given in Table II. For all simulations, the motor characteristics will be utilized as below:

Stator phase resistance Rs (ohm)	= 4.3
Armature Inductance (H)	= 0.0001
Flux linkage established by magnets (V.s)	= 0.05
Voltage Constant (V_peak L-L / krpm)	= 18.138
Torque Constant (N.m / A_peak)	=0.15
Inertia, friction factor, pole pairs [J (kg.m^2)]	=0.000183
Friction factor F (N.m.s)	= 0.001
Pole pairs p( )	=2
Initial conditions[wm(rad/s) thetam(deg) ia,ib(A)]=	[0,0, 0,0]
Sampling Time (Sec)	=1

Table. 2: PMSM parameters

The Matlab, Simulink model of PCC and PTC methods with PMSM using 15-level inverter shown in fig.3 and fig.4. To achieve a comparison between the two methods, the external PI speed controllers are configured with the same parameters. The results of the PCC method and the PTC method with PMSM using 15-level inverter is shown in fig.5, fig.6 compared with the simulation results of the PCC method and the PTC method with IM using 15-level inverter shown in Fig.7, Fig.8 [10]. From the pictures, we can see that both methods have good and similar behaviors at this point in the operation. The PCC method has a slightly better current response; however, the torque ripples of the PTC method are lower than those of the PCC method. The performances in the whole speed range are investigated in the simulations. The motor rotates from positive nominal speed to negative nominal speed. During this dynamic process, the measured speed, the torque, and the stator current are observed. It is clear that both methods have very similar waveforms. They each have almost the same settling time to complete this reversal process due to the same external speed PI parameters. The torque ripples of the PTC method are slightly lower than those of the PCC method. From these simulations, we can conclude that two methods can work well in the whole speed range and have good behaviors with the full load at steady states.

In this paper, switching losses minimization technique through THD minimization. Total harmonic distortion (THD) has calculated successfully in this article by using MATLAB 2013. The proposed scheme shows better response as compared to the conventional one in terms of Total Harmonic Distortion (THD) in speed, torque, and stator current during transient conditions. Fig. 5 (a), (b), (c) and Fig.6 (a), (b), (c) represent the corresponding speed, torque and stator current response of the PTC and PCC schemes using PMSM with a 15-level inverter. The THD in speed, electromagnetic torque and stator current in the PCC and PTC using PMSM with 15-level inverter is shown in Fig.9(a),(b),(c) and Fig.10 (a), (b), (c) respectively. Similarly Fig. 7(a), (b), (c) and Fig.8 (a), (b), (c) represent the corresponding speed, torque and stator current response of the PTC and PCC schemes with a 15-level inverter using IM. The THD in speed, electromagnetic torque and stator current in the PCC and PTC method with IM using 15-level inverter is shown in Fig.11(a), (b), (c) and Fig.12 (a), (b), (c) respectively. It can be compared that, the THD in speed, torque, and stator current with PCC is approximately 5.3% reduces while with PTC is approximately 4.8% reduces in the conventional scheme as per article [10]. In the proposed scheme with 15-level inverter, the THD in speed, torque and stator current with PCC is approximately 23% reduces while, with PTC is approximately also 23 % reduces, which proves the superiority of the proposed PCC and PTC scheme with 15-level inverter over the conventional one compare to article [10] [23] shown in Table.3.

B.PCC and PTC method with PMSM and IM using2-level inverter:

The Matlab, Simulink model of PCC and PTC methods with PMSM using 2-level inverter shown in fig.3 and fig.4. To achieve a comparison between the two methods, the external PI speed controllers are configured with the same parameters. The simulation results of the PCC method and the PTC method with PMSM using 2-level inverter is shown in fig.13(a),(b),(c) and fig.14 (a),(b),(c) compared with the simulation results of the PCC method and the PTC method with IM using 2-level inverter shown in Fig.15 (a),(b),(c), Fig.16 (a),(b),(c) respectively [10]. From the pictures, we can see that both methods have good and similar behaviors at this point in the operation. The PCC method has a slightly better current response; however, the torque ripples of the PTC method are lower than those of the PCC method. The performances in the whole speed range are investigated in the simulations. The motor rotates from positive nominal speed to negative nominal speed. During this dynamic process, the measured speed, the torque, and the stator current are observed. It is clear that both methods have very similar waveforms. They each have almost the same settling time to complete this reversal process due to the same external speed PI parameters. The torque ripples of the PTC method are slightly lower than those of the PCC method. From these simulations, we can conclude that two methods can work well in the whole speed range and have good behaviors with the full load at steady states.

In this paper, switching losses minimization technique through THD minimization. Total harmonic distortion (THD) has calculated successfully in this article by using MATLAB 2013. The proposed scheme shows better response as compared to the conventional one in terms of Total Harmonic Distortion (THD) in speed, torque, and stator current during transient conditions. Fig. 13 (a), (b), (c) and Fig.14 (a), (b), (c) represent the corresponding speed, torque and stator current response of the PTC and PCC schemes using PMSM with a 2-level inverter. The THD in speed, electromagnetic torque and stator current in the PCC and PTC using PMSM with 2-level inverter is shown in Fig.17(a),(b),(c) and Fig.18 (a), (b), (c) respectively. Similarly Fig. 15(a), (b), (c) and Fig.16 (a), (b), (c) represent the corresponding speed, torque and stator current response of the PTC and PCC schemes using IM with a 2-level inverter. The THD in speed, electromagnetic torque and stator current in the PCC and PTC method a 2-level inverter is shown in Fig.19(a), (b), (c) and Fig.20 (a), (b), (c) respectively. It can be compared that, the THD in speed, torque, and stator current with PCC is approximately 5.3% reduces while with PTC is approximately 4.8% reduces in the conventional scheme as per article [10]. In the proposed scheme with 2-level inverter, the THD in speed, torque and stator current with PCC is approximately 19% reduces while, with PTC is approximately also 36 % reduces, which proves the superiority of the proposed PCC and PTC scheme with 2-level inverter over the conventional one compare to article [10] [23] shown in Table.2.

Both the PTC and PCC methods are most useful direct control methods with PMSM method gives 10% to 30% more torque than an induction motor also not require modulator [3]. Induction motor work on only lagging power factor means it can produce only 70-90% of torque produced by PMSM with same current. Total harmonic distortion (THD) has calculated successfully in this article by using MATLAB 2013 compare to (10). The PCC and PTC method with 15-level H-bridge multilevel inverter using PMSM reduces 23% more THD in torque, speed and stator current compared to PCC and PTC method with 15-level H-bridge multilevel inverter using an induction motor shown detail in Table.3 [21]. The graphical representation of % THD in rotor speed, electromagnetic torque and stator current also shown in graph-1,2,3. The comparative issues between PCC and PTC also shown in Table.4. Switching losses are minimized because the transistors are only switched when it is needed to keep torque and flux within their bounds. The switching pattern of semiconductor switches used to get better performance of multilevel inverter. This scheme decreases the switching loss and also increases the efficiency & reduced

losses. In this paper, the PTC and PCC methods with 15-level H-bridge multilevel inverter using PMSM and IM are carried out by simulation method; gives excellent torque and flux responses, robust, and stable operation achieved compared to the PTC and PCC methods with 2-level voltage source inverter, Direct torque control of induction motor (DTC) and Direct torque control of induction motor with fuzzy logic controller (DTC with fuzzy). This novel method attracted the researchers very quickly due to its straightforward algorithm and good performances both in steady and transient states. The proposed scheme shows better response as compared to the conventional one in terms of ripple in speed, torque and stator current during transient conditions [10].

Fig.5: PCC with 15- MLI PMSM Result

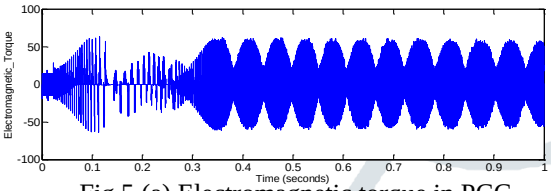

Fig.5.(a) Electromagnetic torque in PCC

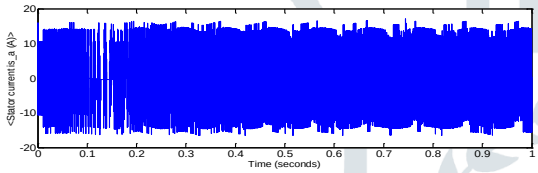

Fig.5.(b) Stator current in PCC

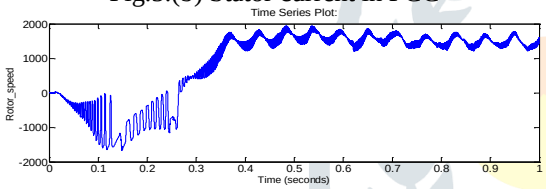

Fig.5.(c) Rotor speed in PCC

Fig.6: PTC with 15-MLI PMSM result

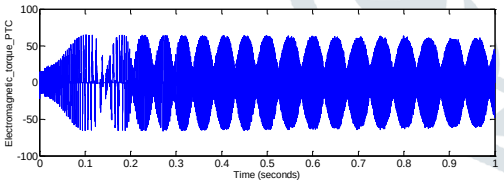

Fig.6.(a) Electromagnetic torque in PTC

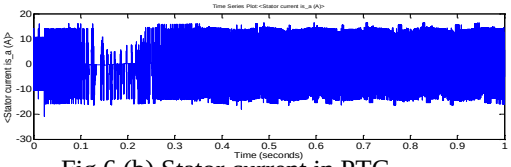

Fig.6.(b) Stator current in PTC

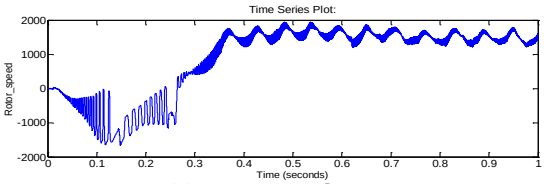

Fig.6.(c) Rotor speed in PTC

Fig.7: PCC with 15-level MLI using IM

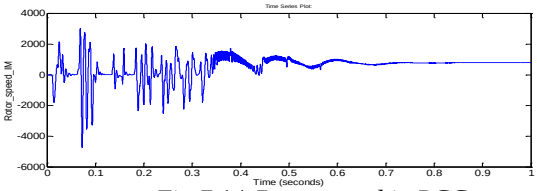

Fig.7.(a) Rotor speed in PCC

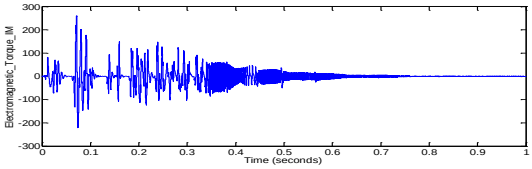

Fig.7.(b) Electromagnetic torque in PCC

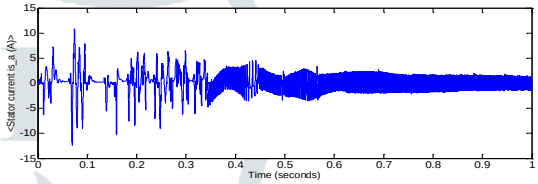

Fig.7.(c) Stator current in PCC

Fig.8: PTC with 15-level MLI using IM result

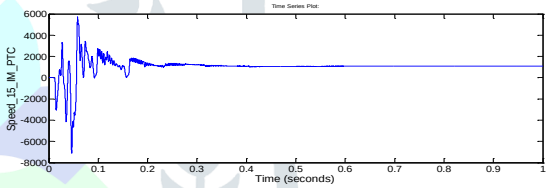

Fig.8.(a) Rotor speed in PTC

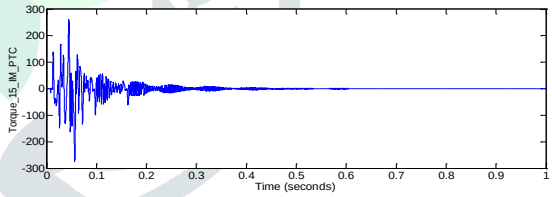

Fig.8.(b) Electromagnetic torque in PTC

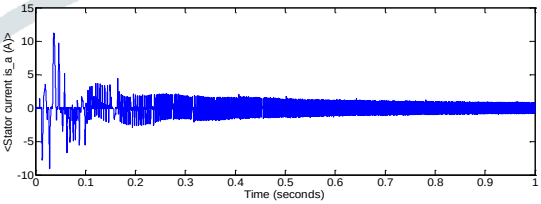

Fig.8.(c) Stator current in PTC

Fig.9: THD in PCC with 15-level MLI using PMSM result

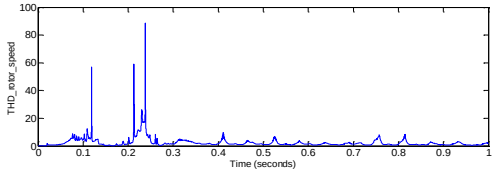

Fig.9.(a) THD in rotor speed

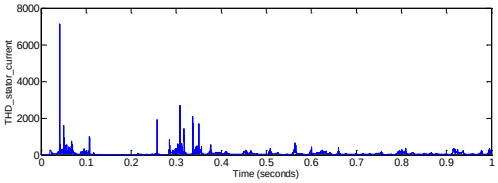

Fig.9.(b) THD in stator current

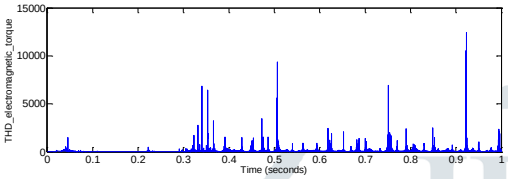

Fig.9.(c) THD in Torque

Fig.10: THD in PTC with 15- MLI using using PMSM

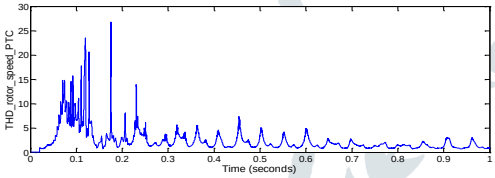

Fig.10.(a) THD in rotor speed

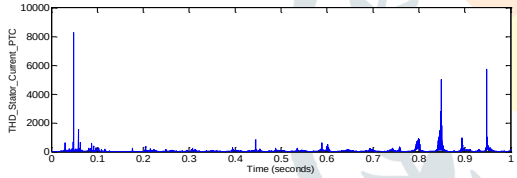

Fig.10.(b) THD in stator current

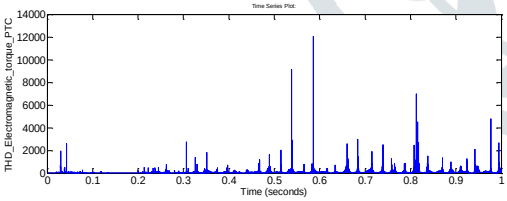

Fig.10.(c) THD in Torque

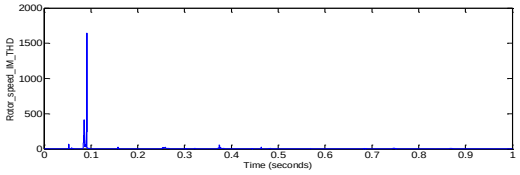

Fig.11.(a) THD in Rotor speed

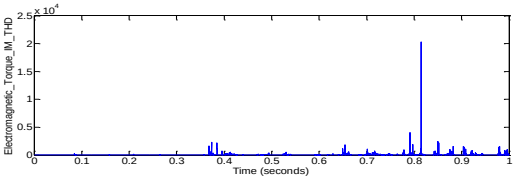

Fig.11.(b) THD in Torque

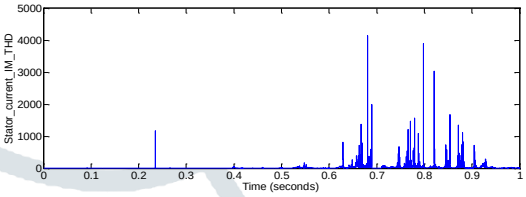

Fig.11.(c) THD in stator current

Fig.12: THD in PTC with 15- MLI using IM

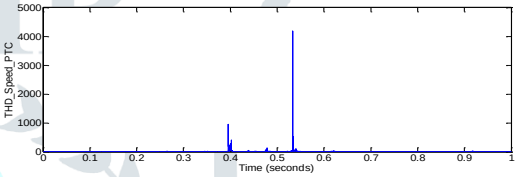

Fig.12.(a) THD in rotor speed

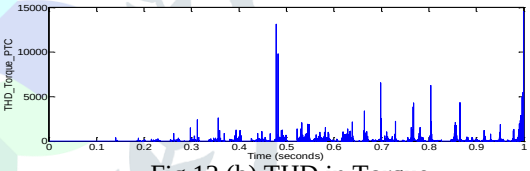

Fig.12.(b) THD in Torque

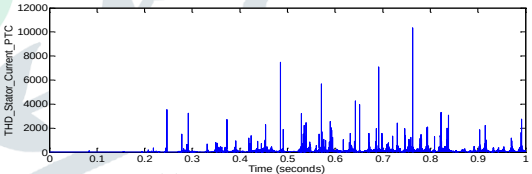

Fig.12.(c) THD in stator current

Fig.11: THD in PCC with 15-level MLI using IM

Fig.13: PCC with 2-level VSI using PMSM

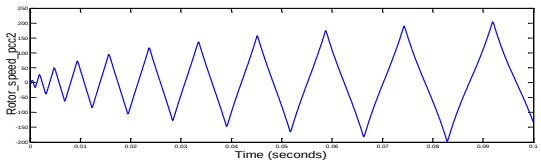

Fig.13 (a) Rotor speed in PCC

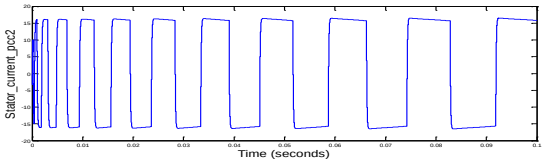

Fig.13 (b) Stator current in PCC

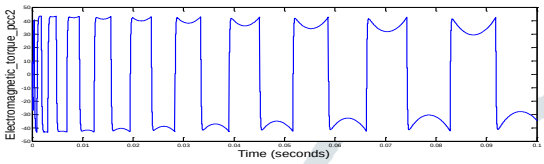

Fig.13(c) Obtained torque in PCC

Fig.14: PTC with 2-level VSI using PMSM

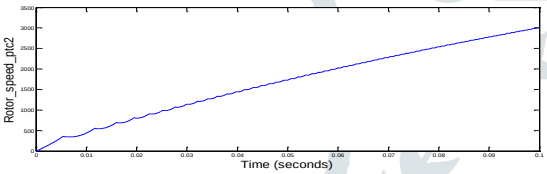

Fig.14 (a) Rotor speed in PTC

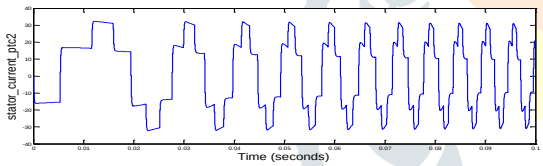

Fig.14 (b) Stator current in PTC

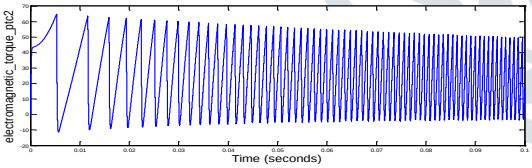

Fig.14 (c) Obtained torque in PTC

Fig.15: PCC with 2-level VSI using IM

Fig.15 (a) Rotor speed in PCC

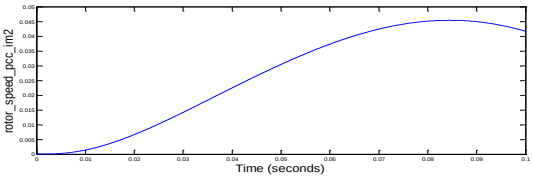

Fig.15 (b) Stator current in PCC

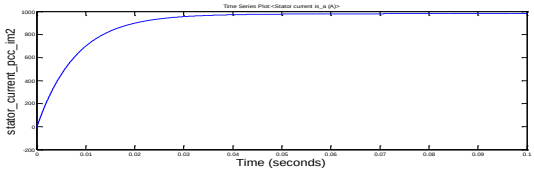

Fig.15(c) Obtained torque in PCC

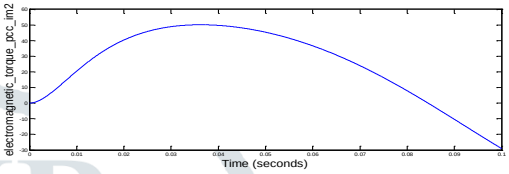

Fig.16: PTC with 2-level VSI using IM

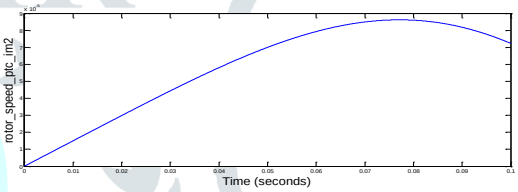

Fig.16 (a) Rotor speed in PTC

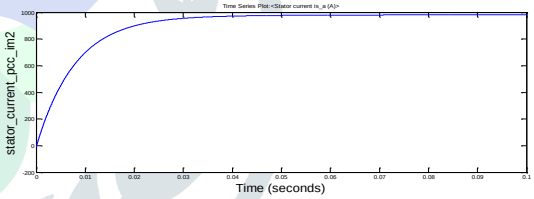

Fig.16 (b) Stator current in PTC

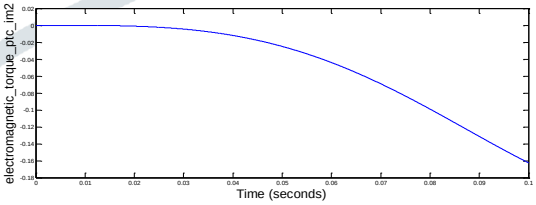

Fig.16 (c) Obtained torque in PTC

Fig.17: THD in PCC with 2-level VSI using PMSM

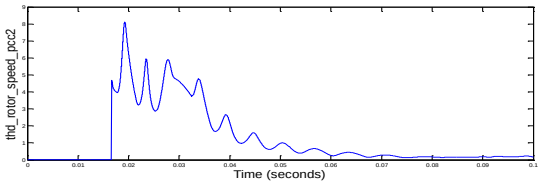

Fig.17 a) THD in rotor speed

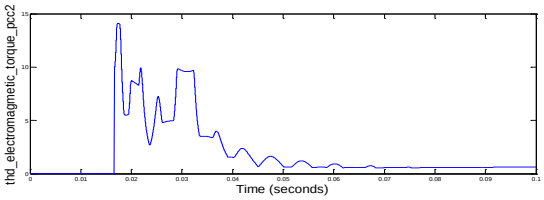

Fig.17(b) THD in electromagnetic torque

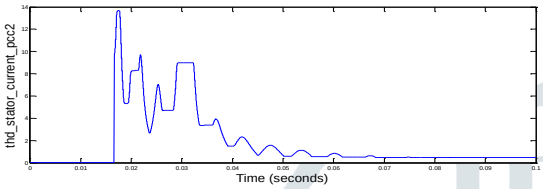

Fig.17 (c) THD in stator current

Fig.18: THD in PTC with 2-level VSI using PMSM

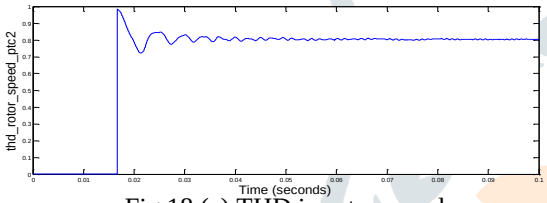

Fig.18 (a) THD in rotor speed

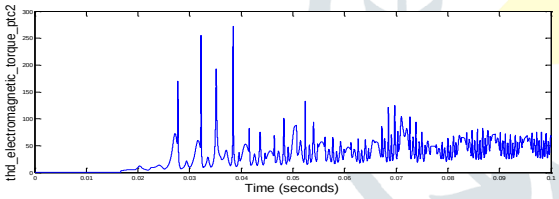

Fig.18(b) THD in electromagnetic torque

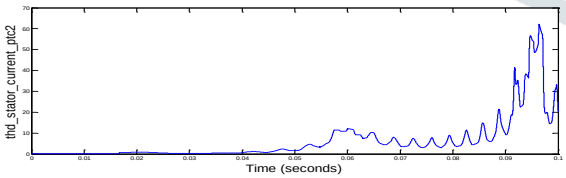

Fig18 (c) THD in stator current

Fig.19: THD in PCC with 2-level VSI using IM

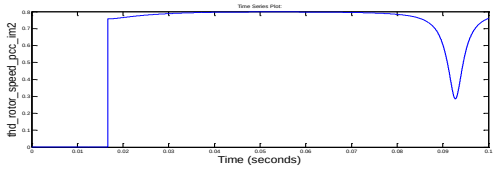

Fig.19 (a) THD in rotor speed

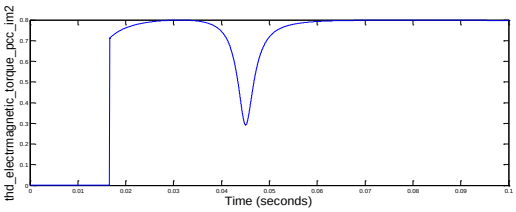

Fig.19 (b) THD in electromagnetic torque

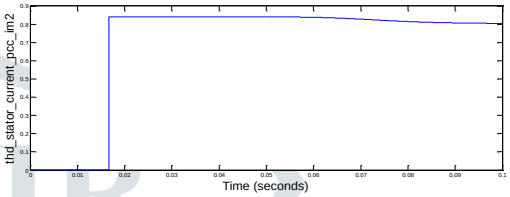

Fig.19 (c) THD in stator current

Fig.20: THD in PTC with 2-level VSI using IM

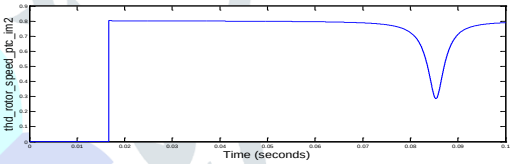

Fig.20 (a) THD in rotor speed

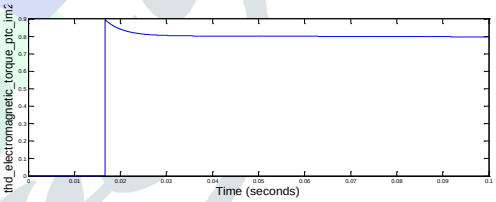

Fig.20 (b) THD in electromagnetic torque

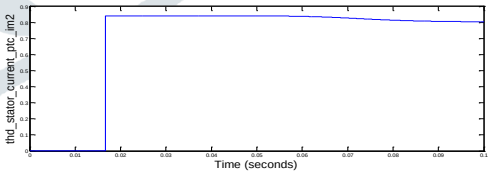

Fig.20 (c) THD in stator current

C.THD Analysis of PCC and PTC method:

Sr. No	Different Methods	%THD in		
		Rotor Speed (w_r)	Torque (T_e)	Stator Current

Feature	PCC	PTC
Conceptual Complexity	Low	Low
PI-current controller	No	No
Use of PWM	No	No
Switching Frequency	Variable	Variable
Dynamics	Fast	Fast
Torque Ripple	Higher	Lower
Stator current THD	Lower	Higher
System Constraints Inclusion	Easy	Easy

D.Comparative Issues between PCC and PTC:

Table.4: Comparative issues between PCC and PTC

E.Graphical Representation of % THD in Speed,Torque and stator current:

a.Graph-1: % THD in Stator

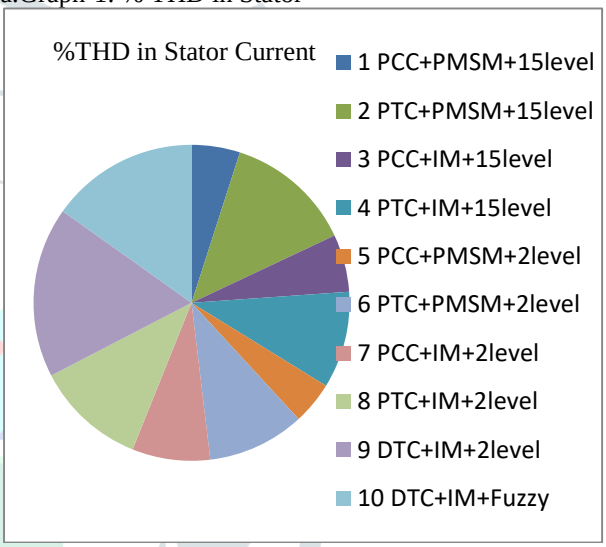

b.Graph-1: % THD in Torque

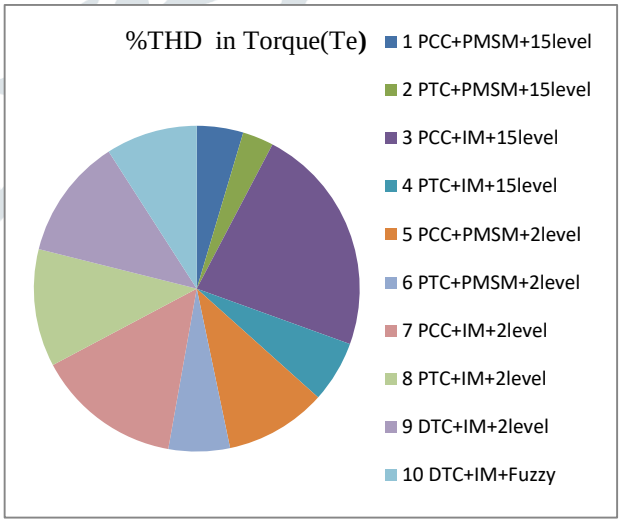

1	PCC with PMSM using 15-level multilevel inverter	31.44	31.34	44.85
2	PTC with PMSM using 15-level multilevel inverter	21	21	118
3	PCC with IM using 15-level multilevel inverter	54.24	155.2	53.22
4	PTC with IM using 15-level multilevel inverter	41.51	41.51	89.67
5	PCC with PMSM using 2-level voltage source inverter(VSI)	82.45	68.60	39.39
6	PTC with PMSM using 2-level voltage source inverter(VSI)	106.11	41.40	90.02
7	PCC with IM using 2-level voltage source inverter(VSI)	118.86	98.14	72.21
8	PTC with IM using 2-level voltage source inverter(VSI)	57.20	79.38	102.34
9	Direct Torque control of IM using 2-level voltage source inverter(VSI)	49.53	81.62	157.84
10	Direct Torque control of IM with Fuzzy Logic Controller using 2-level voltage source inverter(VSI)	49.53	61.82	137.14

Table.3: %THD Calculation comparison

c.Graph-1: % THD in rotor speed

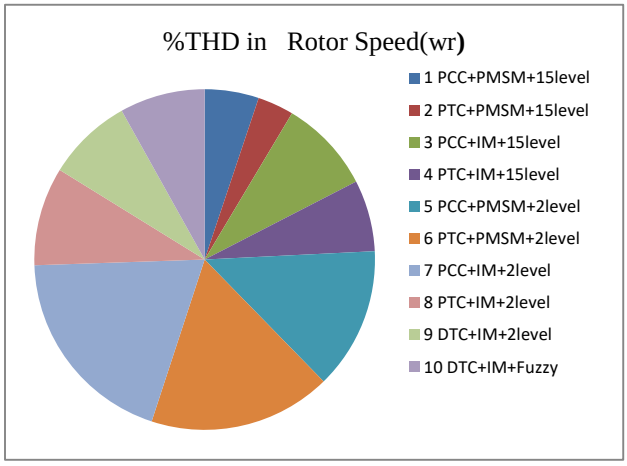

VIII.CONCLUSION

In this paper, PCC and PTC methods of MPC family with 15-level multilevel inverter have been presented and discussed by simulation method only. PCC and PTC methods with 15-level multilevel inverter are direct control methods without an inner current PI controller or a modulator, the PCC method with 15-level multilevel inverter has lower calculation time than the PTC method with 15-level multilevel inverter, fast dynamic response, and Lower stator current harmonics than PTC. This advantage makes the PCC method more accurate for applications with longer prediction horizons. From the test results, it is clear that the PCC method and the PTC method with 15-level multilevel inverter have very good and similar performances in both steady and transient states. PTC method with 15-level multilevel inverter has lower torque ripples; however, the PCC method with 15-level multilevel inverter is better when the currents are evaluated. This novel method attracted the researchers very quickly due to its straightforward algorithm and good performances both in steady and transient states. Future work is to test switched reluctance motor, and servo motor with multilevel inverter is applied to PCC and PTC method, we can imagine that the PCC algorithm and PCC algorithm will greatly reduce the calculation time. The PCC method shows strong robustness with respect to the stator resistance; however, the PTC method shows much better robustness with respect to the magnetizing inductance.

REFERENCES

[1] Patricio Cortés, Marian P. Kazmierkowski, and Ralph M. Kennel, Daniel E. Quevedo, and José Rodríguez, "Predictive Control in Power Electronics and Drives," IEEE Transactions On Industrial Electronics, VOL. 55, NO. 12, Dec. 2008

[2] Georgios Papafotiou, Jonas Kley, Kostas G. Papadopoulos, Patrick Bohren, and Manfred Morari, "Model Predictive Direct Torque Control—Part I: Implementation and Experimental Evaluation," IEEE Transactions On Industrial Electronics, VOL. 56, NO. 6, JUNE 2009

[3] Georgios Papafotiou, Jonas Kley, Kostas G. Papadopoulos, Patrick Bohren, and Manfred Morari, "Model Predictive Direct Torque Control—Part II: Implementation and Experimental Evaluation," IEEE Transactions On Industrial Electronics, VOL. 56, NO. 6, JUNE 2009

[4] Thomas Burtscher and Tobias Geyer, "Deadlock Avoidance in Model Predictive Direct Torque Control," IEEE Transactions On Industry Applications, Vol. 49, No. 5, September/October 2013.

[5] Tobias Geyer, "Model Predictive Direct Torque Control: Derivation and Analysis of the State-Feedback Control Law," IEEE Transactions On Industry Applications, Vol. 49, No. 5, September/October 2013

[6] James Scoltock, Tobias Geyer and Udaya K. Madawala, "A Comparison of Model Predictive Control Schemes for MV Induction Motor Drives," IEEE Transactions On Industrial Informatics, Vol. 9, No. 2, May 2013

[7] Yongchang Zhang and Haitao Yang, "Model Predictive Torque Control of Induction Motor Drives With Optimal Duty Cycle Control," IEEE Transactions On Power Electronics, Vol. 29, No. 12, December 2014

[8] Fengxiang Wang, Zhenbin Zhang, S. Alireza Davari, Reza Fotouhi, Davood Arab Khaburi, José Rodríguez, and Ralph Kennel, "An Encoderless Predictive Torque Control for an Induction Machine With a Revised Prediction Model and EFOSMO," IEEE Transactions On Industrial Electronics, Vol. 61, No. 12, December 2014

[9] Petros Karamanakos, , Peter Stolze, *Student Member*, Ralph M. Kennel, Stefanos Manias, and Hendrik du Toit Mouton, "Variable Switching Point Predictive Torque Control of Induction Machines," IEEE Journal Of Emerging And Selected Topics In Power Electronics, Vol. 2, No. 2, June 2014

[10] Fengxiang Wang, *Member, IEEE*, Shihua Li, *Senior Member, IEEE*, Xuezhu Mei, Wei Xie, *Member, IEEE*, José Rodríguez, *Fellow, IEEE*, and Ralph M. Kennel, *Senior Member, IEEE*, "Model-Based Predictive Direct Control Strategies for Electrical Drives: An Experimental Evaluation of PTC and PCC Methods," IEEE Transactions On Industrial Informatics, Vol. 11, No. 3, June 2015

[11] Md. Habibullah, *Student Member, IEEE*, and Dylan Dah-Chuan Lu, *Senior Member, IEEE*, "A Speed-Sensorless FS-PTC of Induction Motors Using Extended Kalman Filters," IEEE Transactions On Industrial Electronics, Vol. 11, No. 3, Aug 2015

[12] Takahashi and T. Noguchi, "A new quick-response and high-efficiency control strategy of an induction motor," IEEE Trans. Ind. Appl., vol. 22, no. 5, pp. 820–827, Sep. 1986.

[13] I. Takahashi and Y. Ohmori, "High-performance direct torque control of an induction motor," IEEE Trans. Ind. Appl., vol. 25, no. 2, pp. 257–264, Mar./Apr. 1989.

[14] M. Morari and J. Lee, "Model predictive control: Past, present and future," Comput. Chem. Eng., vol. 23, no. 4, pp. 667–682, 1999.

[15] J. Holtz and S. Stadtfeldt, "A predictive controller for the stator current vector of AC machines fed from a switched voltage source," in Proc. IEEE Int. Power Electron. Conf. (IPEC), Mar. 27–31, 1983, vol. 2, pp. 1665–1675.

[16] R. Kennel and D. Schöder, "A predictive control strategy for converters," in Proc. IFAC Control Power Electron. Elect. Drives, 1983, pp. 415–422.

[17] M. Preindl and S. Bolognani, "Model predictive direct torque control with finite control set for PMSM drive systems, part 1: Maximum torque per ampere

operation," IEEE Trans. Ind. Informat., vol. 9, no. 4, pp. 1912–1921, Nov. 2013.

[18] M. Preindl and S. Bolognani, "Model predictive direct torque control with finite control set for PMSM drive systems, part 2: Field weakening operation," IEEE Trans. Ind. Informat., vol. 9, no. 2, pp. 648–657, May 2013.

[19] C. Rojas et al., "Predictive torque and flux control without weighting factors," IEEE Trans. Ind. Electron., vol. 60, no. 2, pp. 681–690, Feb. 2013.

[20] J. Rodriguez *et al.*, "State of the art of finite control set model predictive control in power electronics," *IEEE Trans. Ind. Informat.*, vol. 9, no. 2, pp. 1003–1016, May 2013. [17] J. Rodriguez *et al.*, "Predictive current control of a voltage source inverter," *IEEE Trans. Ind. Electron.*, vol. 54, no. 1, pp. 495–503, Feb. 2007.

[21] P. Correa, M. Pacas, and J. Rodriguez, "Predictive torque control for inverter-fed induction machines," *IEEE Trans. Ind. Electron.*, vol. 54, no. 2, pp. 1073–1079, Apr. 2007.

[22] Padmanaban Sanjeevikumar, "Analysis and Implementation of Multiphase- Multilevel Inverter for Open-Winding Loads", Almamater Studiorum University of Bologna, March 2012, Bologna, Italy

[23] Suraj Karpe, Sanjay.A.Deokar,Arati M.Dixit,"Switching Losses Minimization by Direct Torque Control,"JESIT ,vol.3,December 2016.